Polarity of neutral glycolipids, gangliosides, and sulfated lipids in MDCK epithelial cells

Guy E. Nichols,* Takayuki Shiraishi,† and William W. Young, Jr.†

Departments of Biochemistry* and Pathology,† University of Virginia Medical Center, Charlottesville, VA 22908

Abstract Confluent monolayers of MDCK (Madin-Darby canine kidney) cells provide a widely used model system for studying epithelial cell polarity. We determined the polarity of epithelial cell plasma membrane glycolipids and sulfated lipids by analyzing the lipids released from both sides of monolayers of metabolically labeled MDCK cells. These lipids were released either as endogenously shed material or in budding viruses. All of the glycolipids were detected in both the apical and basolateral domains of the plasma membrane. However, galactosylceramide was more basally oriented than any of the other glycolipids; thus, the ratio of glucosylceramide to galactosylceramide was more than twice as great in the apical domain as in the basolateral domain. A sulfated sterol, which comigrated with cholesterol sulfate, was released in a more basally polarized manner than any of the glycolipids. These results indicate the presence of mechanisms which can produce different degrees of polarity for specific lipids in polarized epithelial cells. **—Nichols, G. E., T. Shiraishi, and W. W. Young, Jr.** Polarity of neutral glycolipids, gangliosides, and sulfated lipids in MDCK epithelial cells. *J. Lipid Res.* 1988. **29:** 1205–1213.

Supplementary key words glycosphingolipid • sterol sulfate

A complex pattern of intracellular traffic is involved in transporting proteins from common sites of synthesis to separate final destinations (1). In polarized epithelial cells, this sorting results in the formation of discrete apical and basolateral domains of the plasma membrane, each of which has a distinct protein composition (2). Currently, an intense research effort is beginning to reveal the mechanisms responsible for the generation and maintenance of this protein polarity (3). Since the vehicles responsible for the transport of proteins to their final destinations are believed to be lipid vesicles (2), it is of interest to determine whether the lipids of polarized epithelial cells are themselves distributed in the plasma membrane in a polarized fashion.

The Madin-Darby (MDCK) canine kidney epithelial cell line has been widely used as a model system for studying epithelial polarity because it has retained many of the characteristics of functional epithelia (2). We recently reported on the polarity of the Forssman glycolipid in MDCK cells (4). In the present report we characterized the release of labeled glycolipids from polarized MDCK cells, either in the form of endogenously shed material or in budding viruses. The rationale for the latter approach was based on an extensive literature (reviewed in refs. 5 and 6) which indicated that, in general, the lipids of most enveloped viruses closely resemble the lipids of the cellular membrane at which they mature. Thus, van Meer and Simons (7, 8) used influenza virus and vesicular stomatitis virus (VSV), which bud exclusively from the apical and basolateral surface of MDCK cells, respectively (9), to determine the phospholipid composition of those domains. Our current results provide evidence that galactosylceramide is more basally oriented than the other major glycolipids of MDCK cells. In addition, a sulfated sterol was released into the basal medium in a more basally polarized manner than any of the glycolipids.

MATERIALS AND METHODS

Cells

Clone BG11 cells were derived from high passage (strain II) MDCK cells and cultured as previously described (10). Sources, methods of preparation of stocks, and titers of stocks of vesicular stomatitis virus (VSV) and the influenza A virus strain PR8 have been described (4). The WSN strain of influenza virus was kindly donated by Dr. E. Rodriguez-Boulan, Cornell University Medical Center. A stock of WSN grown in MDCK cells was concentrated by the polyethylene glycol method (11) and had a titer of 2.2×10^7 PFU/ml.

Abbreviations: MDCK, Madin-Darby canine kidney; VSV, vesicular stomatitis virus; PD, potential difference; TLC, thin-layer chromatography; HPTLC, high performence TLC.

Glycolipid shedding and virus production

Cell growth on filter-bottom cups, metabolic labeling with [^{3}H]galactose and $H_2{}^{35}SO_4$, measurement of transepithelial potential differences (PD), harvesting of labeled glycolipids from the 150,000 *g* pellets and supernatants of culture media, and infection of labeled cell monolayers with viruses were all performed as previously described (4, 10). Virally infected monolayers were incubated at 31°C with 0.2% BSA in DMEM until PD measurements indicated the beginning of loss of monolayer integrity due to the viral cytopathic effect (8 hr for VSV, 14 hr for WSN, and 24 hr for PR8). At these times apical and basal media were harvested. We previously described the methods for virus purification and also provided evidence for polarized viral budding and effectiveness of these purification methods (4). Briefly, correct polarity of viral budding from labeled cells was indicated by a 16-fold higher level of [^{3}H]galactose in the total lipid extract of the PR8 viral pool from the apical medium as compared to the comparable fractions from the basal medium and an 18-fold higher level for the WSN pool. In contrast, the VSV pool from the basal medium contained 5.7-fold more radioactivity than the apical counterpart. SDS-PAGE analysis of the proteins in the viral pellets purified by the procedures described above indicated that all of the major protein bands represented viral proteins.

Glycolipid analysis

Detailed procedures for the isolation and characterization of MDCK glycolipids were described previously (10). The lyophilized supernatants from labeled culture media were extracted in 30 ml of chloroform–methanol 2:1 (v/v) with stirring at 4°C for at least 48 hr followed by reextraction with an Omni mixer (Sorvall, Dupont, Wilmington, DE) once in chloroform–methanol 2:1 (v/v) and twice in chloroform–methanol 1:2 (v/v). Purified glycolipid samples were separated on HPTLC plates (Merck, Darmstadt, FRG) in solvent A (chloroform–methanol–0.25% $CaCl_2$ (aqueous) 60:40:9 (v/v) or solvent B (chloroform–methanol–acetone–glacial acetic acid–water 60:12:24:12:6 (v/v), the latter for separation of sulfated lipids (12). Total lipids were visualized with primuline (13). Glycolipid standards were visualized by resorcinol spray for gangliosides followed by orcinol for total glycolipids. Radiolabeled TLC bands were visualized by autoradiography with fluorographic enhancement (Enhance spray, New England Nuclear) using Kodak XAR-5 film. Glycolipid standards were purified using established procedures (14), except that sulfated lactosylceramide was kindly donated by Dr. David Roberts, NIH. Dehydroepiandrosterone 3-sulfate and sulfatide were purchased from Sigma Chemical Co. Cholesterol sulfate was purchased from Steroloids, Inc., Wilton, NH. Labeled glycolipid bands were quantitated by scraping into scintillation vials and counting in the presence of 10 ml ACS scintillation fluid (Amersham, Arlington Heights, IL).

Glucosyl- and galactosylceramides were separated using the following modification of published methods (15, 16). Glass-backed HPTLC plates were immersed in 2.5% sodium borate in methanol for 10 sec, dried, and activated by heating for 1 hr at 110°C. Chromatography was performed in solvent C (chloroform–methanol–water 62:22:3 (v/v). The densities of orcinol-labeled bands were quantitated as previously described (10).

Distribution of radioactivity into sugar residues of glycolipids was determined by acid hydrolysis and TLC using the following modifications of a published method (17). Glycolipid aliquots were hydrolyzed in 0.5 ml of 3 M HCl at 100°C for 2 hr, with 10 nmol each of galactose, glucose, and N-acetylgalactosamine added as carrier. After drying under vacuum, the hydrolyzates were chromatographed by the continuous development method (18) using HPTLC plates (E. Merck, West Germany) in position 4 (next to the most horizontal position) with solvent D (n-propanol–water 90:10 (v/v) and a development time of 3 hr beyond the time at which the solvent reached the top of the tank. Sugar standards were visualized with silver nitrate (19). This chromatographic method produced 1.2 cm separation between the glucose and galactose bands; glucose, R_f 0.72; galactose, R_f 0.57; and galactosamine, R_f 0.12. Areas corresponding to these sugars were visualized by fluorography as described above, scraped from the chromatogram into counting vials, and incubated overnight with 1 ml of water. Radioactivity was then measured after addition of 10 ml of ACS scintillant (Amersham) to each vial.

The relative specific activity of [^{3}H]galactose in glucose and galactose residues of glycolipids was determined as follows. Forssman glycolipid and G_{M3} ganglioside were purified from extracts of BG11 cells labeled with [^{3}H]galactose using Iatrobead column chromatography as previously described (10). Aliquots of these purified glycolipids were acid-hydrolyzed and incorpoation of radioactivity into sugars was quantitated as described above. The ratio of label in glucose to galactose was 0.43 ± 0.03 (mean ± range for duplicate analyses) for G_{M3} ganglioside (theoretical ratio 1.0) and 0.215 ± 0.01 for Forssman (theoretical 0.5); therefore, the incorporation of label into glucose was 43% of that into galactose. This value was used to compare the relative contents of glucosyl ceramide and galactosyl ceramide as described in the Results.

RESULTS

To determine the polarity of the glycolipids of polarized MDCK clone BG11 cells, we compared the glycolipid patterns of high speed pellets and supernatants obtained from the apical and basal media of polarized monolayers

labeled with [^{3}H]galactose. As shown in **Table 1,** the amount of [^{3}H]galactose-labeled glycolipids shed from both sides of the monolayers was roughly 10% of the cellular content for both total neutral and total acidic glycolipids. To rule out the possibility that this material was due to the release of a small number of dead cells from the monolayer, we analyzed the high speed pellets for activity of the basolateral enzyme (Na^+,K^+)-ATPase (2). As we have previously reported (4), the basolateral pellet contained 58.9 ± 2.4% (mean ± SEM; n = 4) of the total (apical plus basolateral) pellet protein. In striking contrast, ($Na^{\circlearrowleft}$,$K^{\circlearrowleft}$)-ATPase activity could only be detected in the basolateral pellet. Thus, the pelleted material had been released in a polarized fashion and was not the product of dead cells.

Patterns of [^{3}H]galactose-labeled glycolipids

The pattern of neutral glycolipids of MDCK clone BG11 cells labeled with [^{3}H]galactose (**Fig. 1,** lane 1) consisted of a major doublet in the ceramide monohexoside region, a single band of ceramide dihexoside, minor bands in the ceramide tri- and tetra-hexoside areas, and a major doublet of the Forssman ceramide pentasaccharide, as we have previously described (10). We further resolved the ceramide monohexoside region into glucosylceramide and galactosylceramide on borate-impregnated plates (**Fig. 2,** lane 1). The ratio of labeled glucosyl ceramide to galactosyl ceramide in the cells was 2.41 (**Table 2**) as determined by scraping TLC bands and counting followed by correction for the relative specific activity of the [^{3}H]galactose label in glucose residues (0.43) compared to that in galactose residues (1.0; see Materials and Methods). This ratio of labeled components was similar to the ratio of the chemical quantities of these two glycolipids of 2.08 ± 0.02 (mean ± range for duplicate measurements) determined by densitometry of orcinol-stained bands. In contrast, Hansson, Simons, and van Meer (20) reported that in strain II MDCK cells over 90% of the ceramide mono-

TABLE 1. Release of labeled glycolipids and sulfated sterols from MDCK clone BG11 cells

	Cell Content[a]	Released Lipids[a]			Percent of Cell Content Released[b]	Polarity[c] (Basal/Total)
		Apical Medium	Basal Medium	Total		
		cpm × 10^{-4}				%
Total neutral glycolipids	236.3	9.3	12.2	21.5	9.6 ± 1.0	54.2 ± 1.0
Ceramide monohexoside	106.4					
Supernatant		0.6	2.4	3.0		73.3 ± 3.6
Pellet		2.1	4.5	6.6		56.9 ± 6.0
Combined		2.7	6.9	9.6	10.3 ± 1.3	62.2 ± 4.3
Glucosylceramide	52.4					
Supernatant		0.4	1.0	1.4		65.0 ± 2.3
Pellet		1.3	1.8	3.1		51.6 ± 5.1
Combined		1.7	2.8	4.5	10.8 ± 2.0	55.7 ± 3.8
Galactosylceramide	47.7					
Supernatant		0.2	1.2	1.4		82.0 ± 2.7
Pellet		0.7	2.2	2.9		71.1 ± 2.5
Combined		0.9	3.4	4.3	10.0 ± 0.6	74.7 ± 2.2[d]
Ceramide dihexoside	26.4	1.4	1.7	3.1	10.4 ± 1.3	54.5 ± 0.9
Forssman	75.0	3.5	3.9	7.4	10.3 ± 2.4	52.0 ± 0.9
Total acidic glycolipids	20.9	1.3	1.4	2.7	11.3 ± 0.9	54.2 ± 2.0
G_{M3} ganglioside	6.6	0.6	0.5	1.1	14.9 ± 0.8	49.1 ± 3.9
Sulfated glycolipids	10.9	0.6	0.7	1.3	11.1 ± 2.1	57.9 ± 1.7
Sulfated sterol	0.58	0.27	1.15	1.4	241.6 ± 20.9	81.0 ± 4.5

[a] BG11 cells were grown in culture on nitrocellulose filters as described in Materials and Methods. Data were obtained by scraping and counting the bands seen in Figs. 1–4 and were not corrected for the relative specific activity of the [^{3}H]galactose label in glucose and galactose residues. Data are for cells labeled with [^{3}H]galactose except for the sulfated sterol which was labeled with $^{35}SO_4$. Data represent the amount of labeled material harvested from three filter-bottom cups, which is equivalent to 1.5 × 10^8 cells. Due to differences in total incorporation of radiolabeled precursors between experiments, data for cell content and released lipids are presented for one representative experiment. In addition to the data presented for the 150,000 *g* supernatants and pellets of ceramide monohexosides, roughly one-third of the released quantity of each glycolipid category was present in the high speed supernatant and two-thirds in the high speed pellet. The ceramide monohexoside data were obtained by scraping this region from a standard HPTLC plate run in solvent A as shown in Fig. 1, while glucosyl- and galactosylceramide data were obtained from borate-impregnated plates as shown in Fig. 2. Sulfated glycolipids means sulfatide plus sulfated ceramide dihexoside as shown in Fig. 3. Values for the minor glycolipid species ceramide trihexoside, globoside, G_{M1}, and higher gangliosides were too low for quantitation.

[b] Mean ± SEM for three separate [^{3}H]galactose labeling experiments. The sulfated sterol values are mean ± range for duplicate analyses from a single labeling experiment. A second labeling experiment produced a labeling pattern identical to that shown in Fig. 4 but was not quantitated.

[c] Mean ± SEM for four separate [^{3}H]galactose labeling experiments. The sulfated sterol values are mean ± range for duplicate analyses from a single labeling experiment.

[d] Galactosylceramide was significantly more basally polarized than any of the other glycolipids analyzed ($P < 0.01$); the differences between groups were evaluated for statistical significance using unpaired Student's *t*-tests.

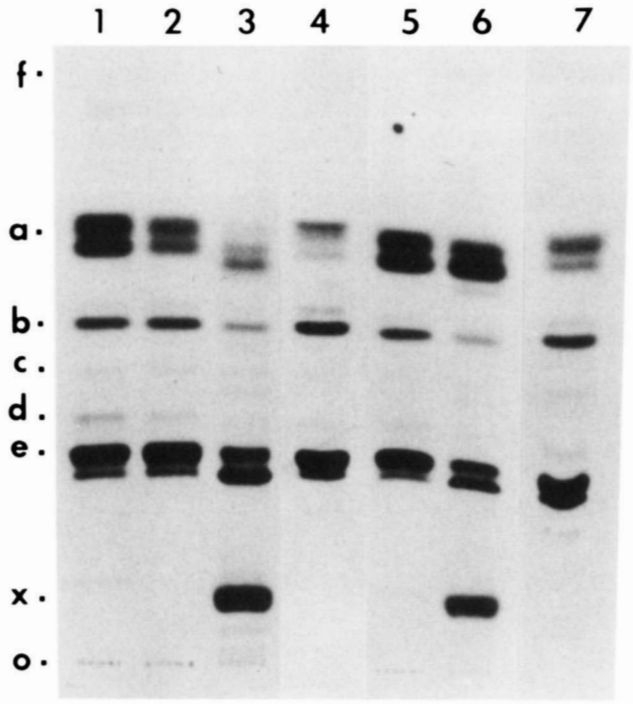

Fig. 1. High performance thin-layer chromatography (HPTLC) pattern of [^{3}H]galactose-labeled neutral glycolipids from MDCK clone BG11 cells. Cells were plated at confluence on nitrocellulose filters and, after generation of a transepithelial potential difference, were labeled with 5 μCi [^{3}H]galactose/ml for 96 hr. Glycolipids from cells, culture media high speed pellets and supernatants, and viruses were isolated and purified as described in Materials and Methods. Aliquots of neutral glycolipids (1000 cpm per lane in lanes 1-3, 5 and 6, 3000 cpm in lane 4, and 500 cpm in lane 7) were separated on an HPTLC plate in solvent A with standards: a) ceramide monohexoside; b) ceramide dihexoside; c) ceramide trihexoside; d) globoside; and e) Forssman. O, origin, f, solvent front. Bands were visualized by fluorography using Enhance spray with exposure to X-ray film at −80°C (30 days for lanes 1-3, 5 and 6; 10 days for lane 4; and 48 days for lane 7). Lanes: 1, cells; 2, apical medium 150,000 *g* pellet; 3, apical medium 150,000 *g* supernatant; 4, influenza strain PR8 purified from the apical medium; 5, basal medium 150,000 *g* pellet; 6, basal medium 150,000 *g* supernatant; and 7, VSV purified from the basal medium. X, nonglycolipid material that could be separated from the labeled glycolipids by chromatography on Sephadex LH-20.

hexoside fraction was galactosylceramide. Thus, clone BG11 and strain II MDCK cells differ markedly in ceramide monohexoside composition, even though the glycolipid patterns of these two cell sources are very similar in other respects, as we previously described (10).

The pattern of neutral glycolipids released into the basal medium during the labeling period and recovered in the high speed pellet (Fig. 1, lane 5) was nearly identical to the cellular pattern. In contrast, the glycolipid patterns of both the high speed pellet and supernatant from the apical medium (Fig. 1, lanes 2 and 3, respectively) were depleted of ceramide monohexosides as compared to the cellular pattern. Similarly, influenza virus PR8, purified from the apical medium following viral infection, also had a reduced level of ceramide monohexosides (Fig. 1, lane 4). The basis of these differences in the ceramide monohexoside region was revealed by chromatography on borate-impregnated TLC plates (Fig. 2). Samples taken from the apical medium, namely the apical pellet, supernatant, and PR8 virus preparations (Fig. 2, lanes 2, 3, and 4, respectively) had reduced contents of galactosylceramide relative to glucosylceramide while galactosylceramide was more abundant in the basolateral pellet, supernatant, and VSV samples (Fig. 2, lanes 5, 6, and 7, respectively). These observation are quantitated in Table 1 and discussed in the following section.

Another major difference in neutral glycolipid patterns between cells and released material was that both the apical and basolateral supernatants (Fig. 1, lanes 3 and 6, respectively) were enriched in the slower migrating band of the Forssman doublet as compared to the patterns of the cells or high speed pellets. We previously reported that the faster Forssman band contained mainly C24 fatty acids while the slower band was composed of C16 and C18 fatty acids (10). Thus, the shedding of Forssman was con-

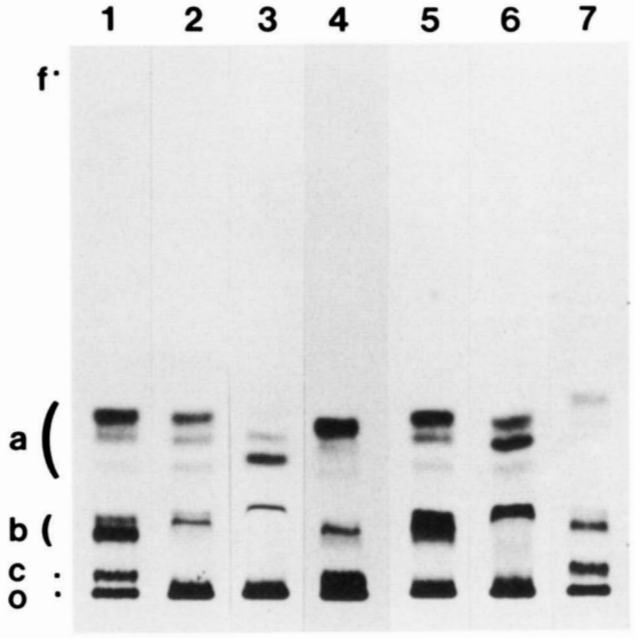

Fig. 2. HPTLC pattern of [^{3}H]galactose-labeled neutral glycolipids from MDCK clone BG11 cells separated on a borate-impregnated plate. Cells were labeled and glycolipids were extracted as described in the legend to Fig. 1. Aliquots of neutral glycolipids (5000 cpm per lane in lanes 1-3, 5, and 6; 3000 cpm in lane 4; and 2000 cpm in lane 7) were separated on a borate-impregnated HPTLC plate in solvent C with standards: 1) glucosylceramide; b) galactosylceramide; and c) ceramide dihexoside. O, origin; f, solvent front. Bands were visualized by fluorography using Enhance spray with exposure to X-ray film at −80°C (9 days for lanes 1-3, 5 and 6; and 21 days for lanes 4 and 7). Lanes: 1, cells; 2, apical medium 150,000 *g* pellet; 3, apical medium 150,000 *g* supernatant; 4, influenza strain PR8 purified from the apical medium; 5, basal medium 150,000 *g* pellet; 6, basal medium 150,000 *g* supernatant; and 7, VSV purified from the basal medium. The mobility of bands in lane 7 was slightly greater than other lanes due to variation in chromatography conditions.

sistent with a pattern that we had previously observed in lymphoma cells (21), namely, the release of less polar species of each glycolipid in a form that could be pelleted while more polar species were enriched in the high speed supernatant (see Discussion). This pattern of supernatant enrichment of more polar glycolipid species was visible in glucosylceramide as well (Fig. 2, lanes 3 and 6). Karlsson, Samuelsson, and Steen (16) indicated that the basis for separation of the three glucosylceramide bands on borate TLC was due to the presence of one free hydroxyl group in the ceramide structure of the fastest band, two in the middle band, and three in the slowest band. We have not determined the lipid composition of these glycolipid species from MDCK cells to date. However, we did verify that each of the three glucosylceramide bands contained only glucose and that the galactosylceramide region contained only labeled galactose (data not shown); this was accomplished by Iatrobead column chromatography and preparative TLC purification of individual bands followed by acid hydrolysis as described in Materials and Methods.

We previously identified (10) the three major acidic glycolipid species of BG11 cells as a major G_{M3} doublet, a sulfatide doublet, and a sulfated ceramide dihexoside doublet (**Fig. 3,** lane 1). The acidic glycolipid patterns of both apical and basolateral high speed pellets were identical to the whole cell pattern (Fig. 3, lanes 2 and 4). The acidic glycolipid patterns of high speed supernatants, however, were relatively enriched in the slower migrating species of both the sulfated lactosylceramide and the G_{M3} doublets (Fig. 3, lanes 3 and 5). Thus, the phenomenon of enrichment in the high speed supernatants of the more polar forms of each glycolipid species extends to acidic as well as neutral glycolipids in MDCK cells.

Quantitation of [^{3}H]galactose-labeled glycolipids

As shown in Table 1, 54% of the total (apical plus basolateral) neutral and acidic glycolipids labeled with [^{3}H]galactose was released into the basal compartment during the labeling period. Among the individual glycolipids analyzed, ceramide dihexoside, Forssman, G_{M3}, and sulfated glycolipids all exhibited a similar pattern of release. In the ceramide monohexoside region, however, galactosylceramide release was significantly more basally oriented than any of the other glycolipids including glucosylceramide (Table 1).

A comparison of the relative quantities of labeled glucosylceramide and galactosylceramide in BG11 cells and samples derived from the apical and basolateral domains is shown in Table 2. The ratio of labeled glucosylceramide to galactosylceramide released from the basolateral membrane was slightly but not significantly reduced from the cell values (Table 2). In striking contrast, the ratios for apically shed glycolipids and for influenza viruses harvested from the apical medium after

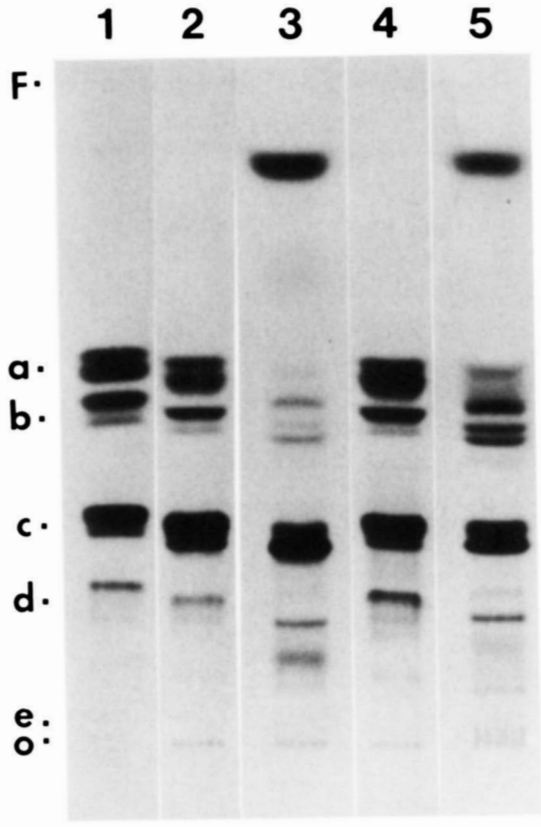

Fig. 3. HPTLC pattern of [^{3}H]galactose-labeled acidic glycolipids from MDCK-BG11 cells. Acidic glycolipids were isolated from cells that were labeled metabolically as described in the legend to Fig. 1. Aliquots of acidic glycolipids (1000 cpm per lane) were separated in solvent A with standards: a) sulfatide; b) sulfated lactosylceramide; c) ganglioside GM3; d) ganglioside GM1; and e) ganglioside GT. Fluorographic exposure was at −80° for 42 days. Lanes: 1, cells; 2, apical medium 150,000 *g* pellet; 3, apical medium 150,000 *g* supernatant; 4, basal medium 150,000 *g* pellet; and 5, apical medium 150,000 *g* supernatant. The unidentified material near the solvent front in lanes 3 and 5 migrated faster than any glycolipid standards.

viral infection were approximately twice as high as the cell values. As shown in Table 1 and **Fig. 4,** all other glycolipids analyzed had patterns of release that were very similar to that of glucosyl ceramide. Thus, the apical domain of BG11 cells was roughly twice as enriched in all other glycolipids relative to galactosylceramide as the basolateral domain.

Release of sulfated sterol

As we have shown previously (10), the sulfolipids of BG11 cells consisted of major sulfatide and sulfated lactosylceramide doublets, and in agreement with the results of Ishizuka et al. (13), included a minor species migrating in the cholesterol sulfate region (**Fig. 5,** lane 1). The patterns of sulfolipids extracted from both apical and basolateral high speed pellets (Fig. 5, lanes 2 and 4) were identical to the cellular sulfolipid pattern. In striking contrast, the high speed supernatants were greatly enriched in a

TABLE 2. Ratio of labeled glucosyl ceramide to galactosyl ceramide in samples from MDCK clone BG11 cells

	Ratio of Glucosyl Ceramide to Galactosyl Ceramide	
Cells	2.41 ± 0.11	(n = 5)
Influenza		
PR8	5.63 ± 0.05	
WSN	3.76 ± 0.5	
Apically released glycolipids		
150,000 *g* Supernatant	5.05 ± 0.4	(n = 4)[a]
150,000 *g* Pellet	4.47 ± 0.35	(n = 4)
Combined	4.61 ± 0.28	(n = 4)
VSV	2.19 ± 0.08	
Basally released glycolipids		
150,000 *g* Supernatant	1.99 ± 0.12	(n = 4)
150,000 *g* Pellet	1.92 ± 0.15	(n = 4)
Combined	1.95 ± 0.13	(n = 4)

Neutral glycolipid samples were prepared from BG11 cells metabolically labeled with [^{3}H]galactose. Data were obtained by scraping and counting the glucosyl- and galactosylceramide bands separated on borate-impregnated TLC plates as shown in Fig. 2. Values represent the mean ± SEM for the number of separate experiments indicated by n, except for the virus values which represent duplicate analyses of one experiment (mean ± range) each for PR8, WSN, and VSV. Glucosylceramide values were corrected for the relative specific activity of [^{3}H]galactose in glucose compared to galactose as described in Materials and Methods. The ratio of labeled glucosylceramide to galactosylceramide in the cells was similar to the ratio of the chemical quantities of these two glycolipids of 2.08 ± 0.02 determined by densitometry of orcinol stained bands.

[a] $P < 0.01$ when comparing combined apically released glycolipids to either cells or combined basally released glycolipids (unpaired Student's *t*-tests). The ratio for basally released glycolipids was not significantly different from that of the cells ($P > 0.05$).

triplet of sulfolipids migrating in the cholesterol sulfate region (Fig. 5, lanes 3 and 5). Although the structure of this apparent sulfated sterol has not been determined as yet, the material comigrated with cholesterol 3-sulfate not only in solvent B, as shown in Fig. 5, but also solvent A (data not shown). The release of this sulfated sterol was more basally polarized than any of the glycolipids, with 81% of the released material being found in the basal compartment (Table 1). Sulfated sterol release also differed from the release of glycolipids in that twice as much sulfated sterol was released into the medium as was present in the cells at the end of the labeling period (Table 1). In addition, approximately 35% of the shed glycolipid label was found in the high speed supernatant, whereas more than 95% of the released sulfated sterol was recovered in the high speed supernatant.

DISCUSSION

In MDCK cells, several plasma membrane proteins have been shown, within the limits of detection of the experimental methods, to be localized exclusively to the basolateral domain whereas apical proteins were less completely polarized (reviewed in ref. 2). In contrast to the examples of strongly polarized proteins, differences in distribution of lipids between apical and basolateral domains of epithelia generally have been less striking; glycolipids in particular have been found to be enriched in the apical domain of several epithelial (summarized in ref. 4). In the present study we characterized the release of labeled glycolipids from polarized MDCK cells, either in the form of endogenously shed material or in budding viruses. These data allow us to estimate the polarity of individual glycolipids in these cells.

von Bonsdorff, Fuller, and Simons (22) reported that the ratio of basolateral to apical membrane areas of

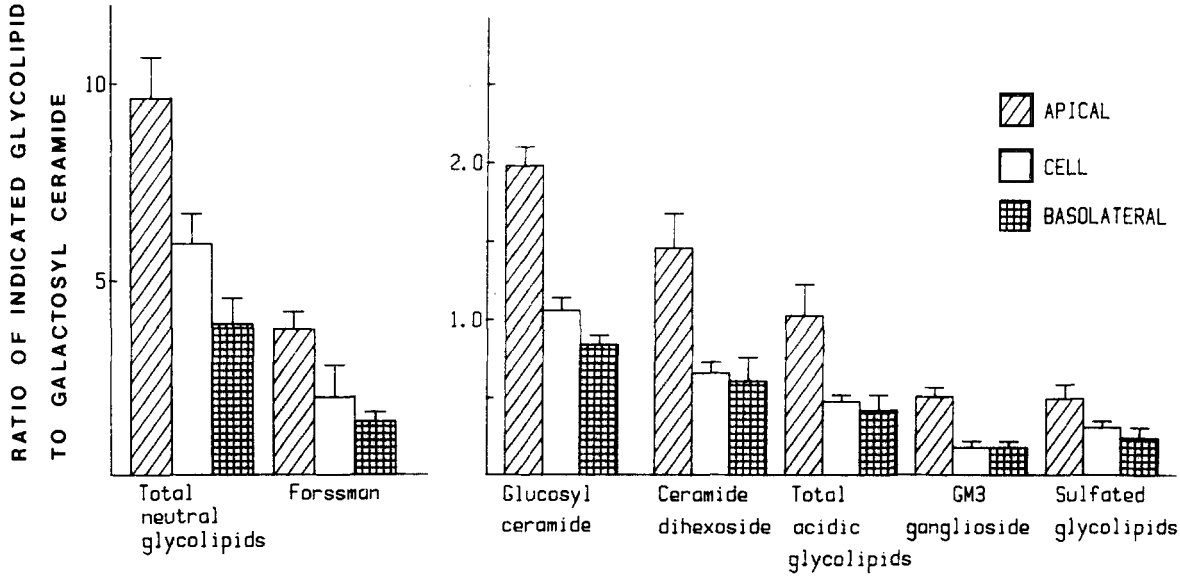

Fig. 4. Ratio of indicated glycolipid to galactosylceramide in clone BG11 cells as compared to the material released into the apical or basolateral culture medium. The apical domain was roughly twice as enriched in all glycolipids relative to galactosylceramide as the basolateral domain. Data presented as the mean values for four separate experiments with the bars representing SEM.

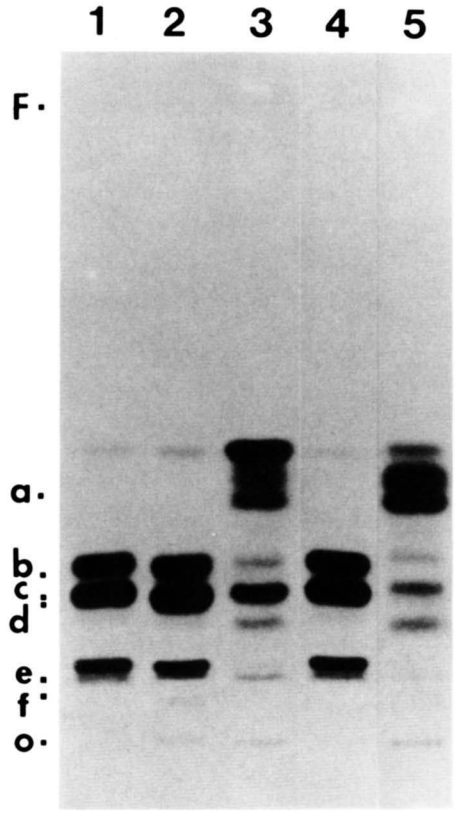

Fig. 5. HPTLC pattern of $^{35}SO_4$-labeled glycolipids. BG11 cells were plated on nitrocellulose filters as described in the legend to Fig. 1 except that the cells were metabolically labeled in medium containing 5 μCi $H_2{}^{35}SO_4$ per ml. Aliquots of total glycolipids (2000 cpm) were separated in solvent B with standards: a) cholesterol sulfate; b) dehydroepiandrosterone 3-sulfate; c) sulfatide; d) ceramide dihexoside; e) sulfated lactosylceramide; and f) ceramide trihexoside. Fluorographic exposure was for 5 days at −80°C. Lanes: 1, cells; 2, apical medium 150,000 *g* pellet; 3, apical medium 150,000 *g* supernatant; 4, basal medium 150,000 *g* pellet; and 5, basal medium 150,000 *g* supernatant.

MDCK strain II cells was four to one. If release of components were strictly proportional to surface area, then 80% of the total released quantity of each nonpolarized component would be found in the basolateral compartment. Thus, from our data in Table 1, galactosylceramide and the sulfated sterol would be considered to be nonpolarized while the concentration of remaining glycolipids would be roughly three- to fourfold higher in the apical than the basolateral domain. However, studies of the secretion of proteins from MDCK cells grown on nitrocellulose filters indicate that a much higher percentage of nonpolarized components is released into the apical compartment than would be predicted from relative surface areas. Kondor-Koch et al. (23) found roughly equal amounts of transfected lysozyme secreted from strain II cells into the apical and basal compartments, whereas Gottlieb et al. (24) reported that for several transfected proteins approximately 60–65% of the total secreted protein was found in the basolateral side of the chamber. As described in the Results, we have found that the high speed pellet from the basolateral culture medium contained 59% of the total (apical plus basolateral) pellet protein. When considered together, these findings suggest that a more realistic figure for release of nonpolarized membrane components would be 60% of the total being found in the basolateral compartment. Based on these latter considerations, galactosylceramide would be strongly polarized ($P < 0.01$) to the basolateral domain while the other glycolipids would be slightly enriched in the apical domain.

Regardless of the above considerations of the definition of quantitative polarity, our data indicate that galactosylceramide is significantly more basally oriented than the other glycolipids studied (Tables 1 and 2 and Fig. 4). Unlike the emerging evidence concerning the mechanisms responsible for protein polarity (3, 25), very little is known about the means by which membrane lipid distributions are generated. One possible mechanism could involve specific proteins that transport or translocate lipids. Cytoplasmic lipid transfer proteins, some of which have specificity for different lipid classes including glycolipids (26–28), could result in the net accumulation of certain lipids in a particular domain. Other proteins, which translocate lipids to the opposite monolayer of the lipid bilayer in the endoplasmic reticulum (29) and in human erythrocytes (30), could markedly effect the distribution of lipids in plasma membrane domains.

Another explanation for the generation of lipid polarity is that lipids partition into different membranes based on the affinity of membrane proteins for specific lipid classes. Several proteins have been shown to exhibit preferential binding to specific lipid classes (31, 32). Thus, the lipid polarity would be a consequence of protein polarity. The observed difference in galactosylceramide polarity could be the result of galactose-specific binding proteins, like the asialoglycoprotein receptor (33), which could direct the distribution of lipids bearing terminal galactose residues.

Alternatively, Coste, Martel, and Got (34) recently showed that in Golgi membranes from porcine submaxillary glands glucosylceramide and glucosyltransferase were oriented on the cytoplasmic surface while glycoprotein galactosyltransferase was on the luminal side. Future studies will be required to determine whether glucosylceramide and galactosylceramide and their synthetic enzymes differ in their orientation in MDCK cells. Such topological differences could be related to the differences in polarity of these glycolipids that we have observed in the present study.

Although shedding of glycolipids from tumor cells has been proposed to be of clinical significance (35), the mechanisms responsible for shedding of membrane components are not well understood (36). We previously showed that glycolipids were shed from mouse lymphoma cells in two forms, one of which was pelleted at high speed, had a high molecular mass ($>40 \times 10^6$ daltons), and had a glycolipid profile identical to that of the cell plasma membrane (21). We concluded that this form

represented membrane vesicles which in the case of MDCK cells could be used as a means of sampling the respective plasma membrane domain from which they were released. The second form remained in the high speed supernatant, was of a size consistent with the glycolipids being bound to plasma proteins, and was enriched in the more polar forms of each glycolipid species (21). With regard to the present studies on MDCK cells, the high speed pellet material may consist of vesicles released from the respective plasma membrane domain. We can only speculate that the high speed supernatant material may result from release of the more polar forms of each lipid species in a nonmembrane bound form, perhaps due to a secretion process.

A sulfated sterol was released from BG11 cells in a more basally polarized manner than any of the glycolipids (Table 1). Based on comigration with cholesterol sulfate in two solvents and the previous identification of cholesterol sulfate in MDCK cells (13), we have tentatively identified this compound as cholesterol sulfate. A variety of functions for cholesterol sulfate have been proposed (37). In most studies cholesterol sulfate has been described as a plasma membrane component (37, 38). However, the pattern of release of the sulfated sterol in our system was very different from that of the glycolipids (Table 1). Twice as much sulfated sterol was released into the medium as was present in the cells at the end of the labeling period. Also, nearly all of the released sterol sulfate was present in the high speed supernatant of the medium. These findings suggest that cholesterol sulfate may be released from MDCK cells in a nonmembrane bound form. Our results may differ from earlier studies because cholesterol sulfate may be more readily released from cells growing on the filters that we used, whereas it may be trapped in the extracellular matrix when released from cells cultured on plastic dishes.

This study was supported by a grant from the Virginia Chapter of the American Heart Association and NIH grant AI-21916. G. E. N. was supported by NIH Medical Scientist Training Program grant GM-07267. We thank Drs. J. C. Brown, W. Gerhard, and E. Rodriguez-Boulan for generous donations of viruses, Dr. D. Roberts for kindly donating the sulfated lactosylceramide standard, C. A. Borgman for excellent technical assistance, and Dr. R. A. Bloodgood for useful comments regarding the manuscript.

Manuscript received 26 January 1988 and in revised form 22 March 1988.

REFERENCES

1. Griffiths, G., and K. Simons. 1986. The trans Golgi network: sorting at the exit site of the Golgi complex. *Science.* **234:** 438–443.
2. Simons, K., and S. D. Fuller. 1985. Cell surface polarity in epithelia. *Annu. Rev. Cell Biol.* **1:** 243–288.
3. Matlin, K. S. 1986. The sorting of proteins to the plasma membrane in epithelial cells. *J. Cell Biol.* **103:** 2565–2568.
4. Nichols, G. E., T. Shiraishi, M. Allietta, T. W. Tillack, and W. W. Young, Jr. 1987. Polarity of the Forssman glycolipid in MDCK epithelial cells. *Biochim. Biophys. Acta.* **930:** 154–166.
5. Lenard, J. 1978. Virus envelopes and plasma membranes. *Annu. Rev. Biophys. Bioeng.* **7:** 139–165.
6. Patzer, E. J., R. R. Wagner, and E. J. Dubovi. 1979. Viral membranes: model systems for studying biological membranes. *CRC Crit. Rev. Biochem.* **6:** 165–217.
7. van Meer, G., and K. Simons. 1982. Viruses budding from either the apical or the basolateral plasma membrane domain of MDCK cells have unique phospholipid compositions. *EMBO J.* **1:** 847–852.
8. van Meer, G., and K. Simons. 1986. The function of tight junctions in maintaining differences in lipid composition between the apical and the basolateral cell surface domains of MDCK cells. *EMBO J.* **5:** 1455–1464.
9. Rodriguez-Boulan, E. and D. Sabatini. 1978. Asymmetric budding of viruses in epithelial monolayers: a model system for study of epithelial polarity. *Proc. Natl. Acad. Sci. USA.* **75:** 5071–5075.
10. Nichols, G. E., J. C. Lovejoy, C. A. Borgman, J. M. Sanders, and W. W. Young, Jr. 1986. Isolation and characterization of two types of MDCK epithelial cell clones based on glycosphingolipid pattern. *Biochim. Biophys. Acta.* **887:** 1–12.
11. Heyward, T., R. Klimas, M. Staff, and J. Obijeski. 1977. The rapid concentration and purification of influenza virus from allantoic fluid. *Arch. Virol.* **55:** 107–119.
12. Ishizuka, I., K. Tadano, N. Nagata, Y. Niimura, and Y. Nagai. 1978. Hormone specific responses and biosynthesis of sulfolipids in cell lines derived from mammalian kidney. *Biochim. Biophys. Acta.* **541:** 467–482.
13. Skipski, V. P. 1975. Thin-layer chromatography of neutral glycosphingolipids. *Methods Enzymol.* **35:** 396–425.
14. Laine, R. A., K. Stellner, and S. Hakomori. 1974. Isolation and characterization of membrane glycosphingolipids. *Methods Membr. Biol.* **2:** 205–247.
15. Kean, E. L. 1966. Separation of gluco- and galactocerebrosides by means of borate thin-layer chromatography. **J. Lipid Res. 7:** 449–452.
16. Karlsson, K. A., B. E. Samuelsson, and G. O. Steen. 1973. The sphingolipid composition of bovine kidney cortex, medulla and papilla. *Biochim. Biophys. Acta.* **316:** 317–335.
17. Fishman, P. H., J. Moss, R. L. Richards, R. O. Brady, and C. R. Alving. 1979. Liposomes as model membranes for ligand-receptor interactions: studies with choleragen and glycolipids. *Biochemistry.* **18:** 2562–2567.
18. Young, W. W., Jr., and C. A. Borgman. 1986. Short bed-continuous development thin-layer chromatography of glycosphingolipids. *J. Lipid Res.* **27:** 120–124.
19. Trevelyan, W. E., D. P. Proctor, and J. S. Harrison. 1950. Detection of sugars on paper chromatograms. *Nature.* **166:** 444–445.
20. Hansson, G. C., K. Simons, and G. van Meer. 1986. Two strains of the Madin-Darby canine kidney (MDCK) cell line have distinct glycosphingolipid compositions. *EMBO J.* **5:** 483–489.
21. Young, W. W., Jr., C. A. Borgman, and D. M. Wolock. 1986. Modes of shedding of glycosphingolipids from mouse lymphoma cells. *J. Biol. Chem.* **261:** 2279–2283.
22. von Bonsdorff, C-H., S. D. Fuller, and K. Simons. 1985. Apical and basolateral endocytosis in Madin-Darby canine kidney (MDCK) cells grown on nitrocellulose filters. *EMBO J.* **4:** 2781–2792.

23. Kondor-Koch, C., R. Bravo, S. D. Fuller, D. Cutler, and H. Garoff. 1985. Exocytotic pathways exist to both the apical and the basolateral cell surface of the polarized epithelial cell MDCK. *Cell.* **43:** 297–306.
24. Gottlieb, T. A., G. Beaudry, L. Rizzolo, A. Colman, M. Rindler, M. Adesnik, and D. D. Sabatini. 1986. Secretion of endogenous and exogenous proteins from polarized MDCK cell monolayers. *Proc. Natl. Acad. Sci. USA.* **83:** 2100–2104.
25. McQueen, N., D. P. Nayak, E. B. Stephens, and R. W. Compans. 1986. Polarized expression of a chimeric protein in which the transmembrane and cytoplasmic domains of the influenza virus hemagglutinin have been replaced by those of the vesicular stomatitis virus G proteins. *Proc. Natl. Acad. Sci. USA.* **83:** 9318–9322.
26. Wirtz, K. W. A. 1982. Phospholipid transfer proteins. *In* Lipid Protein Interactions. Vol. 1. P. C. Jost and O. H. Griffiths, editors. J. Wiley and Sons, New York. 151–231.
27. Wong, M., R. E. Brown, Y. Barenholz, and T. E. Thompson. 1984. Glycolipid transfer protein from bovine brain. *Biochemistry.* **23:** 6498–6505.
28. Yamada, K., A. Abe, and T. Sasaki. 1985. Specificity of the glycolipid transfer protein from pig brain. *J. Biol. Chem.* **260:** 4615–4621.
29. Bishop, W. R., and R. M. Bell. 1985. Assembly of the endoplasmic reticulum phospholipid bilayer: the phosphatidylcholine transporter. *Cell.* **42:** 51–60.
30. Zachowski, A., E. Favre, S. Cribier, P. Herve, and P. F. Devaux. 1986. Outside-inside translocation of aminophospholipids in the human erythrocyte membrane is mediated by a specific enzyme. *Biochemistry.* **25:** 2585–2590.
31. Wiener, J. R., R. Pal, Y. Barenholz, and R. R. Wagner. 1985. Effect of the vesicular stomatitis virus matrix protein on the lateral organization of lipid bilayers containing phosphatidylglycerol: use of fluorescent phospholipid analogues. *Biochemistry.* **24:** 7651–7658.
32. Jones, M. E., and B. R. Lentz. 1986. Phospholipid lateral organization in synthetic membranes as monitored by pyrene-labeled phospholipids: effects of temperature and prothrombin fragment 1 binding. *Biochemistry.* **25:** 567–574.
33. Steer, C. J., and G. Ashwell. 1986. Hepatic membrane receptors for glycoproteins. *Prog. Liver Dis.* **8:** 99–123.
34. Coste, H., M. B. Martel, and R. Got. 1986. Topology of glucosylceramide synthesis in Golgi membranes from porcine submaxillary glands. *Biochim. Bipohys. Acta.* **858:** 6–12.
35. Ladisch, S. 1987. Tumor cell gangliosides. *Adv. Pediatr.* **34:** 45–58.
36. Doljanski, F. 1982. Cell surface shedding. *In* The Glycoconjugates. Vol IV. M. I. Horowitz, editor. Academic Press, New York. 155–190.
37. Rearick, J. I., and A. M. Jetten. 1986. Accumulation of cholesterol 3-sulfate during in vitro squamous differentiation of rabbit tracheal epithelial cells and its regulation by retinoids. *J. Biol. Chem.* **261:** 13898–13904.
38. Bleau, G., F. H. Bodley, J. Longpre, A. Chapdelaine, and K. D. Roberts. 1974. Cholesterol sulfate. I. Occurrence and possible biological function as an amphipathic lipid in the membrane of the human erythrocyte. *Biochim. Biophys. Acta.* **352:** 1–9.